Journal of Power Sources 221 (2013) 228–231

Contents lists available at SciVerse ScienceDirect

Journal of Power Sources

journal homepage: www.elsevier.com/locate/jpowsour

Short communication

Ultra high capacitance values of Pt@RuO_2 core–shell nanotubular electrodes for microsupercapacitor applications

A. Ponrouch, S. Garbarino, E. Bertin, D. Guay*

INRS-Energie, Matériaux et Télécommunications, 1650 Boulevard Lionel Boulet, C.P. 1020, Varennes, QC, Canada J3X 1S2

HIGHLIGHTS

- An array of Pt nanotubes is formed.
- Ruthenium dioxide is deposited in the interior and the exterior of the Pt nanotubes.
- The ruthenium dioxide utilization efficiency is 94.6%.
- The specific geometric capacitance reaches 320mF cm^{-2}.

GRAPHICAL ABSTRACT

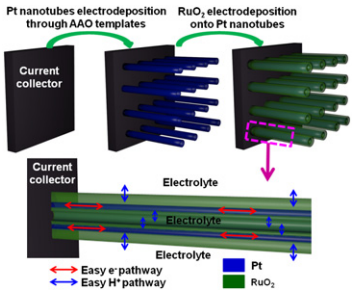

ARTICLE INFO

Article history:
Received 20 June 2012
Received in revised form
10 August 2012
Accepted 13 August 2012
Available online 22 August 2012

Keywords:
Electrodeposition
RuO_2
Supercapacitors
Platinum
Templates
Nanotubes

ABSTRACT

Arrays of Pt@RuO_2 core–shell nanotubes were prepared by electrodeposition of RuO_2 on Pt nanotubes and evaluated as electrochemical microsupercapacitor electrodes. Specific capacitance of *ca.* 1585 and 1280 F $g^{-1}_{RuO_2}$ is obtained at sweep rates of 2 and 500 mV s^{-1}, respectively, demonstrating high utilization factor of RuO_2 due to facilitated transport of protons and electrons. The specific geometric capacitance for the Pt@RuO_2 core shell nanotubes electrode is 320 mF cm^{-2} at 2 mV s^{-1} and 256 mF cm^{-2} at 500 mV s^{-1}.
© 2012 Elsevier B.V. All rights reserved.

1. Introduction

The miniaturization of electronic circuits, sensors and actuators, and the emergence of ambient intelligence through the development of wireless sensor networks, is responsible for a growing demand for compact energy storage elements that can be integrated as close as possible to the electronic circuit they are powering. Moreover, the fabrication of these compact energy storage elements should be compatible with the micro-fabrication processes used to realize the electronic circuits. Micro-batteries offer an attractive alternative for micro energy storage. However, their limited life span is a major problem when they must be integrated in systems with limited access where maintenance and replacement are impossible. In addition, micro-batteries are ineffective for low temperature applications (aerospace) and those requiring high power, as in the case of wireless transmission. In contrast, micro-supercapacitors can store energy in a reversible manner, have fast charge and discharge time (high power) and are able to support thousands of charge and discharge cycles. The

* Corresponding author.
E-mail address: guay@emt.inrs.ca (D. Guay).

0378-7753/$ – see front matter © 2012 Elsevier B.V. All rights reserved.
http://dx.doi.org/10.1016/j.jpowsour.2012.08.033

development of micro-supercapacitors that can quickly and efficiently store and restore energy will positively affect the development of autonomous sensor networks and wireless micro-systems embedded in devices that have application in transportation, home automation, medicine, environment and security.

There are two types of electrochemical capacitors (also called supercapacitors). In the first one, the energy is stored through the accumulation of ions of opposite charge in the double layer of high specific surface area electrodes. Various types of carbon have been used as electrode materials in supercapacitors and some of them have shown promising results when used in microsupercapacitor [1,2]. An interesting way to improve the energy density of microsupercapacitor devices would be to use pseudocapacitive type materials like RuO_2, which have both high specific capacitance (F g^{-1}) and density (g cm^{-3}). Charge storage in RuO_2 involves a change of the Ru oxidation state through the insertion of protons (and electrons) within the bulk of the oxide, thus resulting in specific capacity values that are not limited to the charging of the double layer. Accordingly, the specific capacity value of RuO_2 is 1675 F g^{-1}, considering an optimum stoichiometry of $RuO_2 \cdot 0.5H_2O$ and a redox process involving three electrons over a potential window of 1.2 V [3], resulting in volumetric and geometric energy density far exceeding those of conventional carbon based materials. Large scale applications of ruthenium oxide in (macro)supercapacitors have been prevented because of material cost. However, considering the size of the device and the thickness of the various layers, the amount of materials involved in micro-supercapacitors is limited and cost is mainly determined by the fabrication processes and the assembly of the device. In these conditions, the use of ruthenium dioxide cannot be excluded *a priori*. A more serious concern is the difficulty of maintaining a high specific capacity value as the amount of ruthenium oxide is increased [4,5]. It was shown that this could be achieved by finely dispersing ruthenium oxide to increase its surface area and providing short transport/diffusion path lengths for protons and electrons [6–9]. Using a strategy that was proven successful to improve the power performances of 2D (thin film) micro-batteries [10,11], we propose to rely on the use of a 3D current collector to improve the utilization efficiency and the capacity retention at high discharge rate of ruthenium oxide-based micro-supercapacitor. Here we show for the first time the elaboration of a 3D electrode made of an array of $Pt@RuO_2$ core shell nanotubular structures that display outstanding specific capacitance values even at high sweep rates and which remain stable under potential cycling conditions.

2. Experimental

The aforementioned $Pt@RuO_2$ core shell nanotubular structures were prepared through a simple two steps electrodeposition protocol. First, Pt nanotubes (NTs) were electroplated on Ti substrates from an electroplating solution made of [HCl] = 10 mM and $[Na_2PtCl_6 \cdot xH_2O]$ = 1 mM (Alpha Aesar). Pt NTs were prepared by potentiostatic deposition (E_d = −0.45 V vs SCE, charge density=40 C cm^{-2}) through a porous anodic aluminium oxide (AAO) membrane (Anodisc 25, Whatman International Ltd.) according to a procedure described elsewhere [12–14]. Then, the AAO membrane was dissolved by immersion in 1 M NaOH for 2 h at room temperature. The Pt NTs electrode was then cycled at 50 mV s^{-1} between −0.25 and 1.1 V vs SCE in de-aerated 0.5 M sulphuric acid until a stationary cyclic voltammetric (CV) profile was obtained. The Pt NTs real surface area was evaluated from the CV by determination of the hydrogen desorption charge, using a conversion factor of 210 μC cm_{Pt}^{-2}, and used as current collector for the subsequent electrodeposition of ruthenium oxide.

For the deposition of ruthenium oxide, pre-formed Pt NTs were cycled (400 cycles from −0.25 to 1.1 V at 25 mV s^{-1}) in 5 mM $RuCl_3$ + 10 mM HCl electrolyte [15,16]. These electrodes are denoted as $Pt@RuO_2$ NTs. The RuO_2 loading was determined from the mass difference between the dried Pt NTs electrode (120 °C, for 2 h under vacuum) and the $Pt@RuO_2$ NTs electrode that was previously heat-treated at 150° for 2 h. At this temperature, the balance between electron and proton conduction is optimal [17]. Typical RuO_2 loading was *ca.* 0.20 ± 0.01 mg cm^{-2}.

The electrochemical performances of the $Pt@RuO_2$ NTs electrode were evaluated by CVs measured at various sweep rates. For each sweep rate, a series of 20 CVs were realized to reach steady state and the specific capacitance was computed from the twentieth cycle. All CVs were recorded at room temperature in a three-compartment cell with a Pt gauze and SCE as auxiliary and reference electrode, respectively. De-aerated (Argon N5.0, Praxair) 0.5 M sulphuric acid (A300-212, Fisher Scientific) was used as electrolyte. Deposition and electrochemical characterization were performed using a potentiostat–galvanostat Solartron SI 1287. The morphology of the deposits was observed using a scanning electron microscope (SEM, JSM-6300F, JEOL). The bulk atomic composition was determined by energy dispersive X-ray (EDX) spectroscopy.

3. Results and discussion

First, an array of Pt nanotubes was prepared by Pt electrodeposition through a porous anodic aluminium oxide (AAO) membrane. The choice of Pt as the current collector is justified by the following considerations: (i) its electronic conductivity is high, (ii) it is stable in acidic solution and in the potential window where ruthenium oxide is active, and, most importantly, (iii) it can be processed in the form of an array of nanotubes, providing an ideal conducting, stable support with an extended electrochemically active surface area. It was shown elsewhere that, under the right conditions, Pt nanotubes (NTs) are formed that are firmly attached to the underlying Ti substrate [12–14]. The CV of an array of bare Pt NTs in sulphuric acid solution (see Fig. 1A) displays the typical Pt electrochemical response, with the characteristic proton sorption (between −0.25 and 0.10 V), double layer (between 0.10 and 0.60 V) and Pt oxide formation/reduction (between 0.60 and 1.10 V) potential regions (cf. Fig. 1A, black curve). The real surface area of Pt NTs is *ca.* 80 cm^2 (compared to a geometric surface area of 0.3 cm^2), corresponding to a roughness factor exceeding 250, which is attributed to the hollow 3D character of the array of nanotubes [12–14].

Then it was important to rely on a deposition method that would allow ruthenium oxide to grow evenly on both the interior and the exterior of each Pt NT to maximize the surface area and provide short transport/diffusion path lengths for ions protons and electrons. To achieve this, ruthenium oxide was electrodeposited homogeneously on the surface of Pt NTs by cyclic voltammetry in a $RuCl_3$ containing solution (cf. Fig. 1B). The current intensity increases steadily upon potential cycling, which originates from the continuous growth of an amorphous oxy-hydroxide Ru layer. This process has been studied in detail elsewhere and it involves the adsorption and reduction of a ruthenium species on the negative sweep, followed by its oxidation on the positive sweep [15,16]. The oxide formed at the positive limit is not reduced back to metallic Ru at the negative limit of the potential sweep and the thickness of the oxy-hydroxide Ru deposit increases slowly, as can be judged from the increasing current density observed in Fig. 1B. After 400 potential sweeps, Pt NTs are almost totally covered by oxy-hydroxide Ru, as it can be deduced from the CVs recorded in sulphuric acid (cf. Fig. 1A, red curve), where only a very low contribution originating from proton adsorption/desorption from the

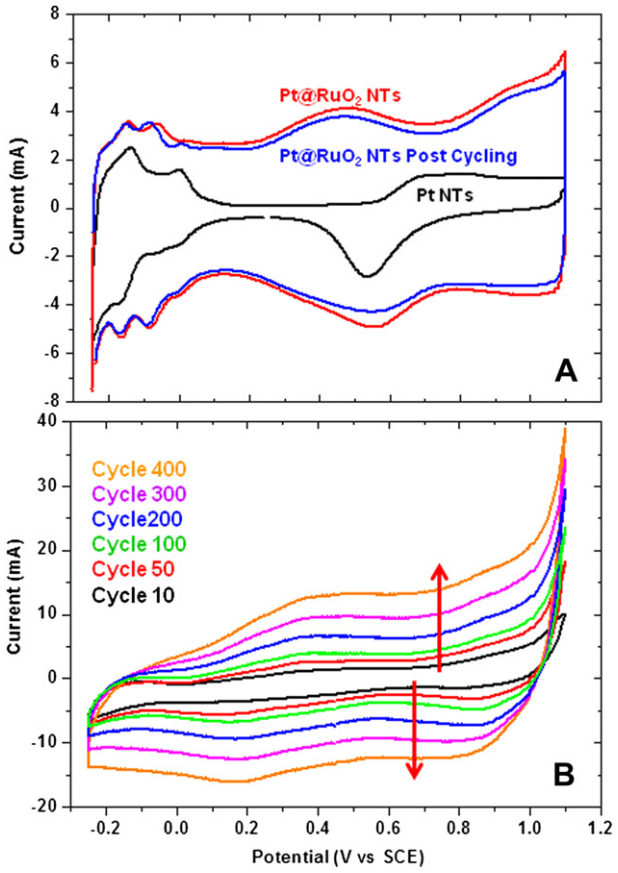

Fig. 1. (A) Cyclic voltammograms (25 mV s^{-1}) in 0.5 M H_2SO_4 for as deposited Pt NT (black curve), as deposited Pt@RuO_2 NT and after more than 200 cycles at various sweep rates (red and blue curves, respectively). (B) Consecutive CV (50 mV s^{-1}) for Pt NT electrode in 5 mM $RuCl_3$ solution. (For interpretation of the references to colour in this figure legend, the reader is referred to the web version of this article.)

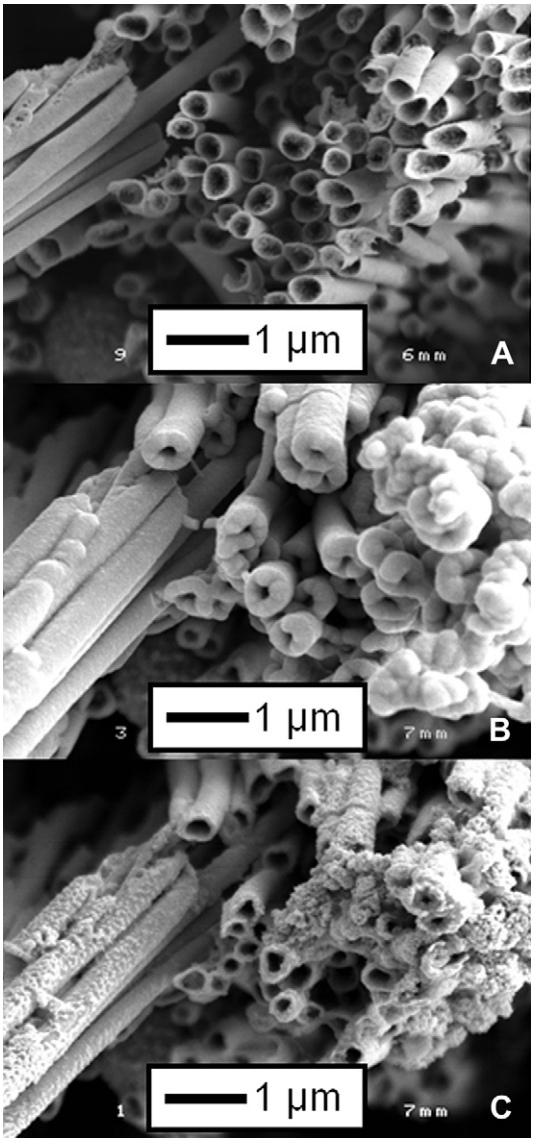

Fig. 2. Scanning electron microscopy micrographs of (A) Pt NT; (B) Pt@RuO_2 NT and (C) Pt@RuO_2 NT following the electrochemical testing procedure.

underlying Pt is still visible (from −0.25 to 0.00 V). In sulphuric acid, the CV for Pt@RuO_2 NT shows an almost rectangular shape, which is the typical electrochemical behaviour of pseudocapacitive amorphous RuO_2 and results from the progressive change in the oxidation state of ruthenium and the diffusion of protons within the bulk of the material. As seen in Fig. 1A, the contribution to the CV originating from the underlying Pt substrate is minimal and does not exceed 2–3% of the total charge observed over the potential window of interest here.

The X-ray diffraction pattern of Pt@RuO_2 NT electrode (not shown) only displays the characteristic diffraction peaks of Pt, indicating that RuO_2 is amorphous. The morphology of oxy-hydroxide Ru deposit onto Pt NTs was examined by SEM. Special care was taken to always analyse the same area of the electrode. As seen in Fig. 2A, 10–20 μm long Pt NTs are initially formed during the electrodeposition of Pt in the AAO membrane. The inner and the outer diameters of the Pt NTs are 280 and 320 nm, respectively, consistent with previous findings [12–14]. Fig. 2B displays the exact same region after RuO_2 deposition. It can be clearly seen that the exterior of the Pt NTs is fully covered by RuO_2 and that deposition of RuO_2 has occurred also in the central (void) region of the NT, leading to the formation of a one-dimensional core shell structure. Consequently, the internal and external diameters of the NT seen in Fig. 2B are 170 and 480 nm, respectively. This highlights that RuO_2 deposition is occurring both on the outside and the inside Pt NTs, resulting in a 20 nm thick Pt NT wall coated with a 135 nm thick RuO_2 deposit (55 nm in the inside and 80 nm on the outside).

In order to evaluate the electrochemical behaviour of these Pt@RuO_2 core shell NT, CVs in H_2SO_4 were performed at various sweep rates ranging from 2 to 500 mV s^{-1} (cf. Fig. 3). The good reversibility of the redox processes occurring in the Pt@RuO_2 core shell NT is revealed by the rectangular shape of the CVs. This reversible behaviour is also present for CVs recorded at 500 mV s^{-1}, indicating excellent proton and electron transport within the electrode. The *y*-axis of Fig. 3 is given in units of d*Q*/d*E* (F g^{-1}). Therefore, the fact that all curves are almost superimposed on each other suggests there is little variation of the capacitance values as the sweep rate is increased. This is further confirmed by computing the specific capacitance, C_s, which is shown in the inset of Fig. 3 as a function of the sweep rates. As seen in the inset, C_s decreases from 1585 to 1280 F $g^{-1}_{RuO_2}$, based on the total amount of RuO_2 deposited, as the sweep rate increases from 2 to 500 mV s^{-1}. At 2 mV s^{-1}, the C_s value represents 94.6% of the RuO_2 maximum theoretical capacitance, indicating that RuO_2 located on the outside and in the inside

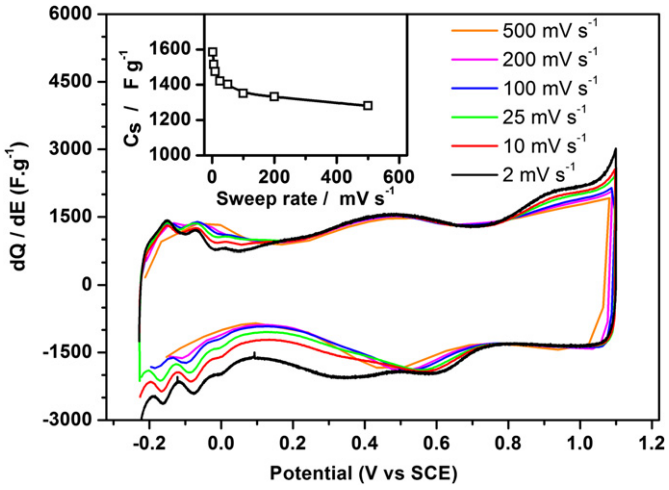

Fig. 3. Cyclic voltammogram of Pt@RuO_2 core shell in 0.5 M H_2SO_4 at sweep rates ranging from 2 to 500 mV s^{-1}. The specific capacitances as a function of the sweep rates are shown in the inset.

of the Pt NT is accessible (*ca.* 30% of the active material being located in the interior of the Pt NT). Following an analysis described in details elsewhere, it is possible to identify two contributions to the total charge (Q_{total}), namely Q_{inner} and Q_{outer}, that are the less and the more easily accessible charge, respectively [18,19]. The contribution of Q_{inner} to Q_{total} is ~5%, consistent with a high utilization of the active material.

To the best of our knowledge, the C_s value recorded at 500 mV s^{-1} (*ca.* 1280 F g^{-1}, which represents >80% capacity retention) is the highest ever reported for RuO_2 based electrodes at such a high sweep rate. Hu et al. [20] reported 60% capacity retention by varying the sweep rate from 10 to 500 mV s^{-1} for an array of self-supported RuO_2 nanotubes. In that later case, the thickness of the RuO_2 layer was only 20 nm as compared to 135 nm in the present study. This clearly demonstrates that maximizing the contact area between the oxide material and the electrolyte, and facilitating ion diffusion in the oxide layer are not enough to reach the highest capacitance values but that the electronic conductivity of the support (metallic Pt) is of paramount importance to achieve discharge rate with excellent capacity retention. This is further confirmed by comparison with the results obtained by Hu et al. with RuO_2 deposited onto TiO_2 nanoflowers, where the specific capacitance does not exceed 545 F g^{-1}, even though the RuO_2 deposit is thinner than 50 nm [21]. The better specific capacitance obtained is most probably due to the higher conductivity of the Pt substrate compared to TiO_2. The specific geometric capacitance for the Pt@RuO_2 core shell NTs is 320 mF cm^{-2} at 2 mV s^{-1} and 256 mF cm^{-2} at 500 mV s^{-1}. At the highest sweep rate, this is a factor *ca.* 150 increase compared to onion-like carbon based micro-supercapacitors [1].

Good electrochemical stability was observed for this type of nanotubular structures. This is evidenced in Fig. 1A, where the CV (at 25 mV s^{-1}) of a native and a cycled Pt@RuO_2 core shell electrode in 0.5 M sulphuric acid (after more than a week and 200 cycles at various sweep rates) are compared. Both curves are almost superimposed on each other, indicating that minor change has occurred during potential cycling, a procedure that mimic the charge/discharge cycles experienced by the electrode during its life span. Indeed, only a small decrease (4.7% loss) of the specific capacitance is observed, that varies from 1421 to 1355 F g^{-1}. This is further confirmed by the SEM micrograph of Fig. 2C that indicates that the RuO_2 deposit is still present on the Pt NT after the electrochemical testing procedure. As far as we can tell, there is no Pt surface exposed, indicating that the adhesion of $RuO_2 \cdot nH_2O$ on the Pt NT is excellent. This is consistent with the bulk composition of the electrode (7 at.% Ru and 93 at.% Pt, evaluated by EDX) that remains constant upon potential cycling.

4. Conclusion

Arrays of Pt@RuO_2 core shell NTs have been prepared using a two steps electro-deposition procedure. At low sweep rate, C_s values as high as 1585 F g^{-1} can be reached, which corresponds to 94.6% utilization efficiency. Also, impressive capacity retention at high sweep rates was observed. These results show that the power capabilities of pseudocapacitive type materials mainly depend on the good electronic contact between the active material and the current collector and that core–shell one-dimensional nanostructure is a very promising avenue for improving micro-supercapacitor performances. We are confident that further improvements can be achieved by tuning the dimensions of such nanostructures (i.e. the length, the inner and outer diameter of the Pt NTs, as well as the thickness of the RuO_2 deposit).

Acknowledgement

This work was made with the financial support of the National Science and Engineering Research Council (NSERC) of Canada and the Canada Research Chair program.

References

[1] D. Pech, M. Brunet, H. Durou, P. Huang, V. Mochalin, Y. Gogotsi, P.L. Taberna, P. Simon, Nat. Nanotechnol. 5 (2010) 651.
[2] D. Pech, M. Brunet, P.L. Taberna, P. Simon, N. Fabre, F. Mesnilgrente, V. Conédéra, H. Durou, J. Power Sources 195 (2010) 1266.
[3] C.C. Hu, W. Chen, K.H. Chang, J. Electrochem. Soc. 151 (2004) A281.
[4] G. Wang, L. Zhang, J. Zhang, Chem. Soc. Rev. 41 (2012) 797.
[5] C.D. Lokhande, D.P. Dubal, O.S. Joo, Curr. Appl. Phys. 11 (2011) 255.
[6] W. Sugimoto, H. Iwata, Y. Murakami, Y. Takasu, J. Electrochem. Soc. 151 (2004) A1181.
[7] W. Sugimoto, K. Yokoshima, Y. Murakami, Y. Takasu, Electrochim. Acta 52 (2006) 1742.
[8] W. Sugimoto, H. Iwata, K. Yokoshima, Y. Murakami, Y. Takasu, J. Phys. Chem. B 109 (2005) 7330.
[9] W. Sugimoto, H. Iwata, Y. Yasunaga, Y. Murakami, Y. Takasu, Angew. Chem. Int. Ed. 42 (2003) 4092.
[10] P.L. Taberna, S. Mistra, P. Poizot, P. Simon, J.-M. Tarascon, Nat. Mater. 5 (2006) 567.
[11] M.M. Shaijumon, E. Perre, B. Daffos, P.L. Taberna, J.-M. Tarascon, P. Simon, Adv. Mater. 22 (2010) 4978.
[12] A. Ponrouch, S. Garbarino, S. Pronovost, P.-L. Taberna, P. Simon, D. Guay, J. Electrochem. Soc. 157 (2010) K59.
[13] A. Ponrouch, S. Garbarino, D. Guay, Electrochem. Commun. 11 (2009) 834.
[14] A. Ponrouch, M.P. Bichat, S. Garbarino, C. Maunders, G. Botton, P.L. Taberna, P. Simon, D. Guay, ECS Trans. 25 (2010) 3.
[15] C.C. Hu, Y.H. Huang, J. Electrochem. Soc. 146 (1999) 2465.
[16] J.-J. Jowa, H.-J. Lee, H.-R. Chena, M.-S. Wu, T.-Y. Wei, Electrochim. Acta 52 (2007) 2625.
[17] C. Sopcic, Z. Mandic, G. Inzelt, M.K. Rokovic, E. Mestrovic, J. Power Sources 196 (2011) 4849.
[18] S. Ardizzone, G. Fregonara, S. Trasatti, Electrochim. Acta 35 (1990) 263.
[19] J. Gaudet, A. Tavares, S. Trasatti, D. Guay, Chem. Mater. 17 (2005) 1570.
[20] C.C. Hu, K.H. Chang, M. Lin, Y. Wu, Nano Lett. 6 (2006) 2690.
[21] C.C. Hu, H.Y. Guo, K.H. Chang, C.C. Huang, Electrochem. Commun. 11 (2009) 1631.